

Integrated Photonic Transceiver for Adaptive Mitigation of Atmospheric Turbulence in Free Space Optical Links

A. Martinez⁽¹⁾, S. Seyedinnavadeh⁽¹⁾, F. Zanetto⁽¹⁾, F. Morandi⁽¹⁾, A. Milani⁽²⁾, A. D'Acerno⁽²⁾, L. Resteghini⁽²⁾, F. Morichetti⁽¹⁾ and A. Melloni⁽¹⁾

⁽¹⁾ Dipartimento di Elettronica, Informazione e Bioingegneria, Politecnico di Milano, Milan, Italy

⁽²⁾ Huawei Technologies Italia Srl, Segrate, Italy

Corresponding author: andrea.melloni@polimi.it

Abstract *We present an adaptive optical transceiver implemented using an integrated programmable optical processor to reduce scintillation effects in Free Space Optical communications. We validated the transceiver performance on intensity-modulated signal at up to 25 Gbaud transmitted through an indoor setup emulating a midrange-distance link. ©2024 The Authors.*

Introduction

Atmospheric turbulence is one of the main obstacles in implementing high-bitrate reliable Free Space Optics (FSO) communication systems [1]. Turbulence introduces a random phase and amplitude perturbation of the wavefront of propagating optical beams, reducing the coupling efficiency with the transceiver and causing a deep fading in the signal after the photodetector [2]. This effect is known as scintillation and can be mitigated by means of adaptive optics, that is, by sampling the distorted beam wavefront at different points where the spatial coherence of the signal is preserved. Since each sample of the beam-front has uncorrelated amplitude and phase (that randomly varies on a time scale of several hundred Hz [3]), the adaptive optical transceiver must combine coherently the spatial samples faster than the coherence time of the channel to recover the spatial coherence of the beam.

In this paper, we report on a self-configuring optical transceiver that consists of a 16-element integrated 2D optical phased array (OPA) and a programmable optical processor (POP) that coherently (re)combines the various portions of the optical beam. In our experiments, such a reconfigurable photonic integrated circuit (PIC) is used either at the receiver side (Rx) or the transmitter side (Tx) of an FSO link. The POP is a binary-tree mesh of thermally tuneable Mach-Zehnder Interferometers (MZIs), with local feedback loops that implement a control algorithm to compensate for the scintillation. Adaptive mitigation of scintillation in free space optical beams is demonstrated on intensity-modulated optical signals at a data rate of up to 25 Gbaud, intentionally distorted by an indoor system emulating the atmospheric turbulence of an FSO link of several hundreds of meters. Experimental results demonstrate the effectiveness of the approach in terms of

performance and footprint compared with other solutions.

FSO integrated transceiver

The integrated FSO transceiver has been designed to generate and receive optical beams with a diameter of around 40 mm (before the collimating optics) or 400 μm at the optical phase array (OPA) surface. The OPA design is optimized to compensate for turbulence with a scintillation index up to $\sigma_I^2 = 10^{-2}$, corresponding to an outdoor link of several hundreds of meters in length. A schematic of the transceiver PIC is shown in Fig. 1. The OPA is composed of 16 surface grating couplers (GCs) with a central GC and the remaining ones arranged in two concentric rings with a radius of 60 μm (inner ring, 7 GCs) and 180 μm (outer ring, 8 GCs), respectively (see Fig. 1(a)). Each CG is about 48 μm -long and 23 μm -wide, with a 24 μm -long taper. The elevation angle of the radiated field is 3°, the azimuth angle is 0°, and the divergence is 5.6°×9.8°. The spacing between GCs was optimized to match the beam's coherence radius r_0 (Fried parameter) in the maximum turbulence conditions.

The POP is a 16x1 binary mesh realized on a commercial Silicon Photonics (SiPh) platform. It is composed of 15 balanced MZI. Each MZI has two actuators (thermal shifters) and an integrated germanium photodetector (PD) placed in one of the output ports (see Fig. 1(a)) that provides a feedback signal to the control loop. The POP is connected through wire bonding to a custom electronic board that minimizes the signal read by the PD (see Fig. 1(b)) In this way, the two optical signals at the input of each MZI are coherently recombined and routed towards a standard waveguide (not connected to a PD), providing the output optical port for fiber coupling [4].

The control system uses a dithering technique, which allows the control of the MZIs of

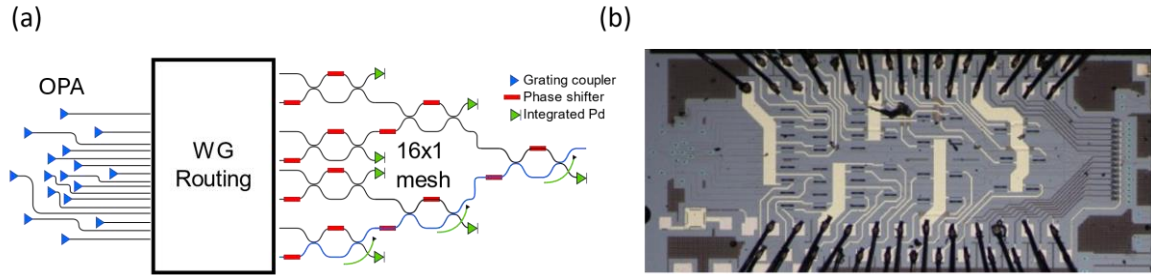


Fig. 1: Schematic of the adaptive FSO transceiver: (a) layout of the integrated FSO transceiver including an Optical Phased Array (OPA) and programmable optical processor (POP) made of a binary tree mesh of thermally tunable MZIs connected to an array of integrated monitor PDs. (c) Top view photograph of the silicon photonic chip wire bonded to an electronic

the mesh with no ambiguity on the direction of tuning to minimize the power at the PDs effectively [5]. This technique implements a lock-in measurement that is frequency and phase-selective. Thus, a single dithering frequency can be used for many actuators, allowing a wider control bandwidth (e.g., to control the 30 heaters, only two dithering frequencies were necessary) [5]. Each actuator can be controlled independently, and all the MZIs can be tuned in parallel. Finally, the coherently recombined signal of the last MZI of the mesh is coupled out using a vertically aligned single-mode fiber.

Experimental Results

To validate the mitigation of turbulence-induced scintillation effects, we built an indoor FSO link emulator [see Fig. 2 Fig. 2(a)]. We used an SMF collimator to assess the reception (Tx forward) and transmission (Tx backward) capabilities of the transceiver PIC under turbulent conditions. The turbulence was emulated using a spatial light modulator (SLM) (15.36 mm x 8.64 mm with a pixel pitch of 8 μ m), introducing a phase screen (PS) in the propagation path of the beam. The PSs were generated to emulate a turbulence strength at several hundred meters of propagation with an effective refractive index parameter C_n^2 within 10^{-13} and 10^{-9} [m^{-2/3}]. An IR camera captured the effects of the SLM on the beam, as seen in Fig. 2(b-d). Panel (b) shows the acquired Gaussian beam (Tx forward) before the SLM, while panel (c) shows the effect on the

Gaussian beam of the phase screen. The phase screen distorts the beam, changing its shape, size, and centroid. Panel (d) shows the POP transmitted beam (Tx backward) before the SLM when the POP is in its native state.

First, system-level measurements were performed for different conditions of the FSO link using an intensity-modulated 5 Gbps signal OOK NRZ. Fig. 3(a) shows the received optical power [collected at the output waveguide of the binary tree POP of Fig. 1(a)] for one phase screen when the adaptive control is OFF and ON. When a perturbation of the FSO beam is introduced with the SLM and the adaptive control is OFF, the average received power of the output port of the integrated POP drops to -27 dBm. In this condition, the signals sampled by the 16 GCs of the OPA interact randomly along the mesh depending on the local phase of the incoming scintillated beam. The effect on the transmitted data can be seen in the acquired eye diagram in Fig. 3(b). When the control is activated [POP ON in Fig. 3(a)], the POP compensates for the relative phase differences between the signals (by minimizing the received power at each integrated monitor photodetector), maximizing the output power. In this case, the average received power is -12 dBm. This result shows that the intensity fading at the output port of the photonic chip is largely compensated, as seen in the wide-open eye of Fig. 3(c). The slight residual fading is because, for different conditions of turbulence (different configurations of the SLM),

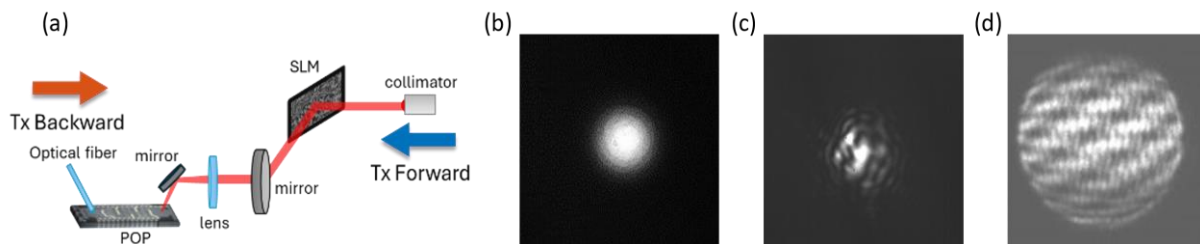


Fig. 2: (a) Schematic of the experimental setup used for the emulation of turbulence-induced scintillation on FSO beams. (b) Photograph of the transmitted beam from the collimator (b) before and (c) after the SLM. (d) Photograph of the far field of the transmitted beam from the POP before the SLM.

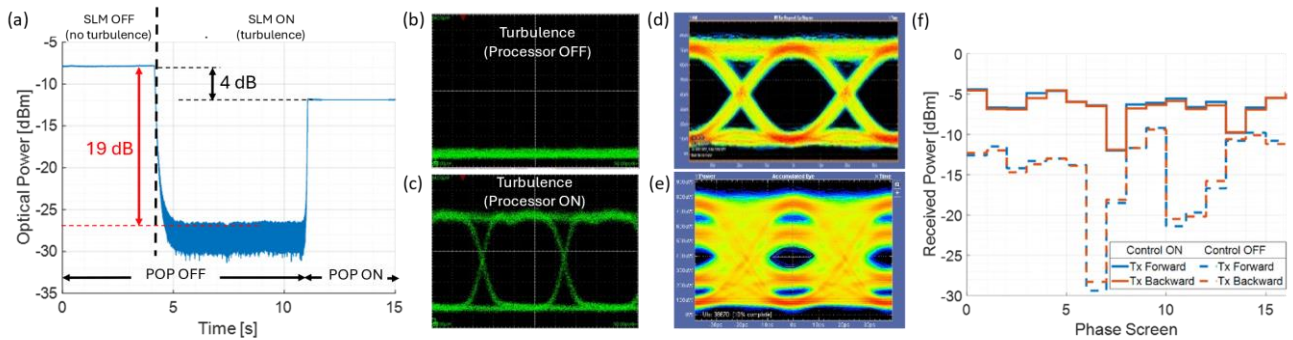


Fig. 3: (a) Optical power of the FSO beam at the output port of the integrated transceiver with a phase screen implemented by the SLM when the adaptive control is OFF and ON. Eye diagrams of a 5 Gbps NRZ modulated signal when the control is (b) OFF and (c) ON. Eye diagrams of a 25 Gbaud (d) NRZ and (e) PAM-4 modulated signals. (f) Received optical power for Tx Forward (blue) and Tx Backward (orange) when the control is ON (solid line) and OFF (dashed line).

some GCs may receive more or less power. Fig. 3 (d) and (e) show the eye diagrams of 25 Gbaud NRZ and PAM-4 modulated signals, respectively, at the output port of the POP, demonstrating the capability of the transceiver to manage wide-band optical signals.

Finally, we validated the capability of the POP used on the Tx side to compensate for turbulence effects as well as the POP on the Rx. Fig. 3(f) shows the received power for Tx Forward (POP Rx, blue line) and Tx Backward (POP Tx, orange) when the control is ON (solid line) and OFF (dashed line) for 16 different phase screens introduced with the SLM. When the control is OFF, the average power is -15 dBm with $\text{std} = 5.28$ dB. Meanwhile, for the control ON, the average power is -6.1 dBm with $\text{std} = 1.77$ dB. The received power is almost the same for both link configurations. To compensate for the power fading caused by the turbulence in both Tx forward and Tx backward, the phase shifts applied to the MZIs (for each PS) were the same. This means that if used as a transceiver, the POP automatically pre-compensates for transmission by compensating the received beam, avoiding the need for a return channel.

Conclusions

In conclusion, we demonstrated the mitigation of scintillation effects induced by indoor-emulated atmospheric turbulence in an FSO link using an integrated adaptive transceiver based on a 2D OPA and a POP. The broad optical band of the transceiver enables the use of signals modulated at a data rate of tens of Gbaud as well as advanced modulation formats. Results show an effective reduction of intensity fading due to beam scintillation effects when the transceiver is used at the Tx or Rx side of the link. Our experiments used scintillation levels as high as those expected in outdoor links of several hundreds of meters. The performance of the proposed transceiver can be improved by increasing the number of optical antennas of the OPA and a

more complex POP, thus enabling the compensation of a higher degree of turbulence and the realization of an FSO link with several km of length.

Acknowledgments

The research has been carried out in the Huawei-Politecnico di Milano Joint Research Lab framework. Part of this work was carried out at Polifab, Politecnico di Milano, Milan, Italy.

References

- [1] Y. Wang, H. Xu, D. Li, R. Wang, C. Jin, X. Yin, S. Gao, Q. Mu, L. Xuan, and Z. Cao. "Performance analysis of an adaptive optics system for free-space optics communication through atmospheric turbulence". Scientific Report 8, 1124 (2018). DOI:<https://doi.org/10.1038/s41598-018-19559-9>.
- [2] X. Zhu and J. Kahn. "Free-space optical communication through atmospheric turbulence channels." IEEE Transactions on Communications 50, 1293 – 1300 (2002). DOI: [10.1109/TCOMM.2002.800829](https://doi.org/10.1109/TCOMM.2002.800829).
- [3] M. A. Cox, N. Mphuthi, I. Nape, N. Mashaba, L. Cheng, and A. Forbes, "Structured Light in Turbulence" in IEEE Journal of Selected Topics in Quantum Electronics, vol. 27, no. 2, pp. 1-21, (2021). DOI:[10.1109/JSTQE.2020.3023790](https://doi.org/10.1109/JSTQE.2020.3023790)
- [4] D. A. B. Miller, "Self-configuring universal linear optical component" Photonics Research 1, 1-15 (2013). DOI:<https://doi.org/10.1364/PRJ.1.000001>
- [5] F. Zanetto, V. Grimaldi, F. Toso, E. Guglielmi, M. Milanizadeh, D. Aguiar, M. Moralis-Pegios, S. Pitris, T. Alexoudi, F. Morichetti, A. Melloni, G. Ferrari, and M. Sampietro. (2021), "Dithering-based real-time control of cascaded silicon photonic devices using non-invasive detectors". IET Optoelectron, 15: 111-120 (2021). DOI: <https://doi.org/10.1049/ote2.12019>